DOT HS-820 227

HOLOGRAPHIC TECHNIQUES FOR NONDESTRUCTIVE TESTING OF TIRES

Contract No. DOT-TSC-NHTSA-72-4

April 1972

Interim Report

U.S. DEPARTMENT OF TRANSPORTATION

NATIONAL HIGHWAY TRAFFIC SAFETY ADMINISTRATION

WASHINGTON, D.C. 20590

The opinions, findings, and conclusions expressed in this publication are those of the authors and not necessarily those of the National Highway Traffic Safety Administration.

1. Report No. DOT/HS-820 227	2. Government Accession No.	3. Recipient's Catalog No. PB-214 258
4. Title and Subtitle HOLOGRAPHIC TECHNIQUES FOR NONDESTRUCTIVE TESTING OF TIRES		5. Report Date April, 1972 6. Performing Organization Code
7. Author(s) Harry L. Ceccon		8. Performing Organization Report No. DOT-TSC-NHTSA-72-4
9. Performing Organization Name and Address U.S. Department of Transportation National Highway Traffic Safety Admin Washington, D.C. 20590		10. Work Unit No. R2402 11. Contract or Grant No. HS203
12. Sponsoring Agency Name and Address U.S. Department of Transportation National Highway Traffic Safety Admin Washington, D.C. 20590		13. Type of Report and Period Covered Interim Report 14. Sponsoring Agency Code
15. Supplementary Notes Details of illustrations in this document may be better studied on microfiche		

16. Abstract

Holographic interferometric techniques were used in a development program to evaluate the feasibility of the technique in the nondestructive testing (NDT) of commercial automobile tires.

Passenger tires with built-in defects were holographically inspected to determine the types of tire defects that can be detected using this method. Separations and voids were located reliably. Defects other than separations and voids were detected in some cases.

A program is currently underway in which "off-the-shelf" passenger tires are first inspected holographically as well as by other NDT methods, then subjected to the Motor Vehicle Safety Standard 109 endurance or high speed tests, reholographed and then sectioned analytically. The objective of the program is to correlate nondestructive test data with tire failure.

17. Key Words	18. Distribution Statement		
Nondestructive Testing of Tires Holographic Testing of Tires	unlimited		
19. Security Classif. (of this report) Unclassified	20. Security Classif. (of this page) Unclassified	21. No. of Pages ~~74~~ 68	22. Price 3.00

PREFACE

Holographic Techniques for nondestructive testing of tires described in this report were used by the Transportation Systems Center, Electromechanical Branch. This work was performed as a part of the Nondestructive Automobile Tire Testing Program sponsored by the Department of Transportation through the National Highway Traffic Safety Administration, Research Institute.

The object of this work was to develop holographic techniques for detecting latent anomalies in automotive tires and determining the relationship of the holographic "signatures" of the anomalies to defects found in the tires. The author acknowledges the assistance received from Mr. A. Lavery, Mr. I. Litant, Mr. T. Kelley, and Mr. A. Scapicchio for their significant contribution to the conduct of this program.

TABLE OF CONTENTS

Section		Page
1.0	INTRODUCTION	1
2.0	REAL-TIME HOLOGRAPHIC STUDY OF RUBBER/CORD SPECIMENS	3
2.1	PROCEDURES	3
2.2	RESULTS	4
2.3	CONCLUSIONS	9
3.0	DOUBLE EXPOSURE HOLOGRAPHIC STUDY OF TIRES PROGRAMMED WITH BUILT-IN DEFECTS	11
3.1	PROCEDURES	11
3.2	RESULTS	12
3.3	CONCLUSIONS	16
4.0	DOUBLE EXPOSURE HOLOGRAPHIC STUDY OF COMMERCIAL "OFF-THE-SHELF" TIRES	30
4.1	PROCEDURES	30
4.2	RESULTS	31
4.3	CONCLUSIONS	35
5.0	DISCUSSION	36
6.0	RECOMMENDATIONS	39
APPENDIX A - REVIEW OF BASIC OPTICAL HOLOGRAPHY AND HOLOGRAPHIC INTERFEROMETRY		A-1
APPENDIX B - REAL-TIME HOLOGRAPHIC INTERFEROMETRIC APPARATUS AND PROCEDURES TO INSPECT CONTROLLED SPECIMENS		B-1
APPENDIX C - DOUBLE-EXPOSURE HOLOGRAPHIC APPARATUS AND PROCEDURES USED TO INSPECT TIRES		C-1
APPENDIX D - GLOSSARY AND SYMBOLS		D-1

LIST OF ILLUSTRATIONS

Figure		Page
1.	Rubber/Cord Control Specimen	3
2.	Holographic Interferogram of Rubber/Cord Specimen with No Defect	4
3.	Holographic Interferogram of Rubber/Cord Specimen with Ply Separation	4
4.	The Effects of Relaxation Time on a Rubber/Cord Specimen with a Separation Defect	5
5.	Pressure Effects on Holographic Interoferograms of a Rubber/Cord Specimen	7
6.	The Effect of Specimen Thickness on Holographic Interferograms of Rubber/Cord Specimens	8
7.	Holographic Interferogram of a Rubber/Cord Specimen with a Broken Cord	9
8.	Holographic Interferogram of a Rubber/Cord Specimen with a Ply Overlap	9
9.	Holographic Interferogram of Tire with No Defects	17
10.	Holographic Interferogram of a Tire With a Separation Between the Tread and Top Belt	18
11.	Holographic Interferogram of a Tire with a Separation Between the Plies and the Belt	19
12.	Holographic Interferogram of a Tire With a Separation in the White Sidewall Area	20
13.	Holographic Interferogram of a Tire With a Separation in the Black Sidewall Area	21
14.	Holographic Interferogram of a Tire with a 1 Inch Separation in the Center of the Tread Area and a 1 Inch Separation in the White Sidewall Area	22
15.	Holographic Interferogram of a Tire With a 1 Inch Separation in the Center of the Tread Area and a 1 Inch Separation in the Black Sidewall Area. Separations were Surrounded by a 12 Inch Weak-Bond Area	23
16.	Holographic Interferograms of 2 Tires Out-Of-Round From Excessive Rubber in the Tread and Shoulder Area	24

LIST OF ILLUSTRATIONS (CONT.)

Figure		Page
17.	Holographic Interferogram of a Tire With an Overlap of 2 Inches in the Second Body Ply Extending from Bead to Bead	25
18.	Holographic Interferogram of a Tire With Second Body Ply Folded Back on Itself for 1 Inch Extending from Bead to Bead	26
19.	Holographic Interferogram of a Tire With Ruptured Cords in the Center of the Tread Area (No Defect Signature)	27
20.	Holographic Interferogram of a Tire With Ruptured Cords in the Shoulder on the Black Sidewall (No Defect Signature)	28
21.	Holographic Interferogram of a Tire With a Permeable Tubeless Inner Liner (No Defect Signature)	29
22.	Section of a Tire (#ϕ1T6061) Carcass With a Ply Separation	32
23.	Holographic Interferogram of Tire (#ϕ1T6061)	32
24.	Section of a Tire (#ϕ1T6142) Carcass With a Tread Separation	33
25.	Holographic Interferogram of Tire (#ϕ1T6142)	33
26.	Irregularities in Gross Fringe Pattern	34
A-1.	Typical Holographic Set-Ups	A-1
B-1.	Real-Time Holographic Interferometer Schematic	B-1
B-2.	Block Diagram of the Real-Time Holographic Interferometric Set-Up	B-2
B-3.	Laboratory Real-Time Holographic Set-Up	B-3
B-4.	Vacuum Chamber and Specimen Holder	B-4
B-5.	Holograms of Rubber/Cord Specimens	B-6
B-6.	Automatic Film Processor and Liquid Gate	B-6
C-1.	GCO PT-12 Holographic Tire Analyzer	C-2

LIST OF ILLUSTRATIONS (CONT.)

Figure		Page
C-2.	Shematic of Optical System of GCO Holographic Tire Analyzer	C-3
C-3.	Tire Prepared for Holographic Inspection	C-4
C-4.	Turn Table and Sidearm Mounts	C-4
C-5.	GCO Holographic Reconstruction Setup	C-5
C-6.	Holographic Interferogram of a Tire with No Defects	C-7
C-7.	Holographic Interferogram of a Tire with a Separation Between the Tread and Top Belt	C-8
C-8.	Holographic Interferogram of a Tire with a Ply Overlap	C-9

1.0 INTRODUCTION

This report documents the use of holographic techniques in detecting latent anomalies in automotive tires and determining the relationship of the holographic "signatures" of these anomalies to defects found in the tires after they were cut into sections and physically examined.

The program was conducted in four phases. In Phase 1, a review of basic optical holography and holographic interferometry was made to establish a baseline for equipment and procedures to be used and techniques to be developed. The review is contained in Appendix A.

In Phase 2, rubber/cord control specimens were fabricated in-house with specific built-in defects and examined using real-time holographic interferometry. The primary purpose of this phase was to develop experience in techniques and to correlate and tabulate characteristic holographic signatures of the known defects. The equipment and techniques used are contained in Appendix B.

In Phase 3, double-exposure holographic techniques were used to examine full size, automobile passenger tires which were custom made with known built-in defects. Holographic interferograms were obtained and the various fringe signatures compared with the known defects. Resultant holographic signatures which were characteristic of the various types of defects were tabulated.

Phase 4 of the program is currently underway and will continue for another year. In this phase, new and retread commercial vehicular tires are purchased "off-the-shelf" in the open market on a random basis. These tires are inspected holographically to locate and identify latent defects. The defects are tabulated and compared with those found when the tires are subsequently cut up and physically examined in detail.

The laboratory setups and procedures used in Phase 3 and 4 are shown in Appendix C.

Findings and conclusions are presented in the body of the report to follow for Phase 2, 3 and 4.

2.0 REAL-TIME HOLOGRAPHIC STUDY OF RUBBER/CORD SPECIMENS

2.1 PROCEDURES

The Materials Laboratory at the Transportation Systems Center (TSC) prepared a series of flat specimens of rubber/cord to provide controlled defects for the calibration of the holographic equipment. The materials used were nylon, polyester or fiberglass tire ply stock, and skim stock (uncured rubber sheeting). Separations were created by pre-curing the rubber in areas of specific size using heated metal cylinders. When the final laminate of two or four layers of the ply stock was made, the cured areas were matched; the heat and pressure used to cure the surrounding rubber did not affect the pre-cured areas. In other cases, powdered talc was used to make the separations between plies by creating non-adhering surfaces. Separation and ply overhap defects were built into the specimens at various locations and depths prior to curing. Ruptured cord defects were created by means of a plunger after the specimens were cured. The control specimens varied in size from 4 to 8 inches square and 0.10 to 0.60 inches in thickness. (See Figure 1)

Figure 1. Rubber/Cord Control Specimen

The samples were mounted in specimen holders and allowed to set a minimum of 30 minutes to reduce creeping of the specimen rubber. The samples were then placed in a vacuum chamber and carefully examined using the real-time holographic technique and the vacuum straining method described in Appendix B.

The objectives for this phase of the holographic study were to determine the following:

1. The types of defects that could be detected.
2. The location and size of the defect.
3. The optimum vacuum straining pressure for each type of defect and sample size and thickness.
4. The extent of correlation between the holographic findings of the defects and the actual defects existing in the control specimens.

2.2 RESULTS

Figure 2 shows an interferogram of a specimen with no defects. Only gross fringes from creeping rubber are visible. Figure 3 is a specimen with a separation in the central area. Concentric rings show the location and size of a separation. The fringe density is an indication of the severity of the separation.

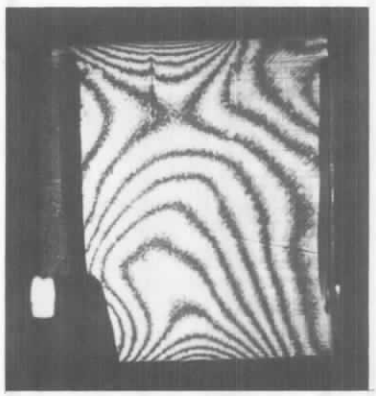

Figure 2. Holograph Interferogram of Rubber/Cord Specimen with No Defect

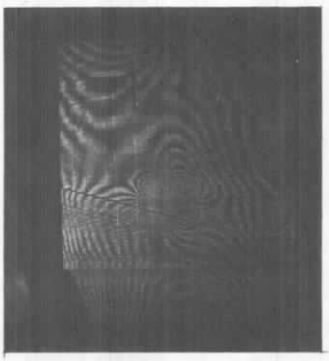

Figure 3. Holographic Interferogram of Rubber/Cord Specimen with Ply Separation

Fringes generated by creeping rubber can add spurious fringe information and should be minimized if possible. Our study showed that for the rubber/cord specimens, 30 minutes relaxation time minimized creep fringes to the point where defect investigation could be performed. Figure 4 shows two interferograms of a specimen that was allowed to set for different time periods before holographing. Figure 4a shows the fringe pattern generated by a 1/2 inch separation in the center of a rubber/cord specimen surrounded by a fringe pattern generated by creeping rubber. This specimen was allowed to relax for one hour before holographing. Figure 4b shows an interferogram of the same specimen taken after it was allowed to relax for 72 hours. The time between

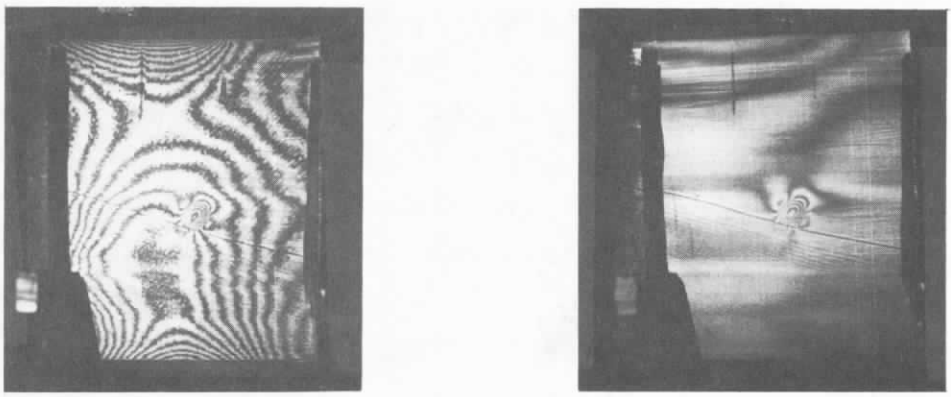

a. 15 torr, 1 hour relaxation time

b. 15 torr, 72 hour relaxation time

Figure 4 The Effects of Relaxation Time on a Rubber/Cord Specimen with a Separation Defect

exposures (hologram and copy camera) was the same in both cases. This example shows that although insignificant creep fringes are present, the fringes generated by the anomaly is easily distinguishable. Relaxation time of 20 to 30 minutes can be tolerated for this type of specimen.

The optimum differential straining pressure required to expose the sub-surface anomalies varied with separation size and with sample thickness. The amount of differential vacuum applied to a defective rubber/cord sample has an effect on the surface displacement and therefore on the fringe signature of that particular defect. Figure 5 shows the effect of applying different vacuum straining pressures to a specimen containing a 1/2 inch diameter separation. The optimum straining pressure for this particular specimen was about 15 torr. Excessive pressures can cause excessive surface displacement and produce an interferogram which has a high unresolvable fringe density. Figure 5 shows that this was the case with the interferogram generated using a differential straining pressure of 40 torr.

Figure 6 shows the effects of vacuum straining pressure on specimens of different thicknesses. Both specimens in Figure 6 contain a 1 inch separation midway between the front and back surfaces. The specimen in Figure 6a is 0.55 inches thick and the specimen in Figure 6b is 0.32 inches thick. A differential straining pressure of 15 torr was used in both cases. As one might expect, the surface displacement of the thicker sample was less. The fringe signal from the thicker sample was two fringes (approximately 1 μ displacement). The signal from the thinner sample was 15 fringes (approximately 5 μ displacement).

The surface displacement caused by subsurface anomalies varied with the diameter of the defect. This was especially true for separations. Surface displacement for large diameter defects was greater than for smaller defects provided that all other conditions were the same.

Attempts were made to detect ply overlaps and broken cords in rubber/cord specimens. Cords ruptured prior to vulcanization

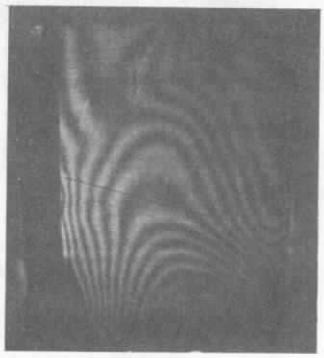

ΔP = 0 TORR

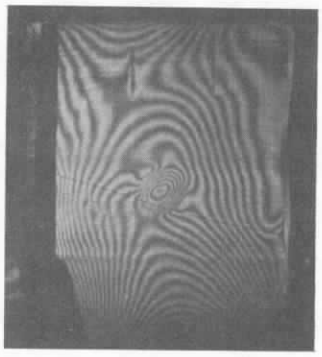

ΔP = 15 TORR

ΔP = 5 TORR

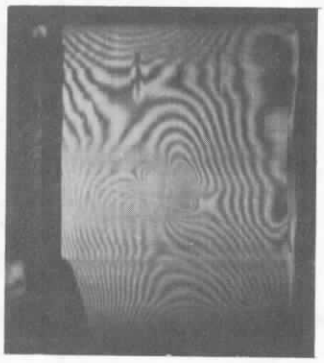

ΔP = 40 TORR

(1/2" Diameter Separation)
(2 ply specimen - 1/8 inch thick)

Figure 5: Pressure Effects on Holographic Interoferograms of a Rubber/Cord Specimen

a. 1 inch separation, 2 ply specimen, 0.55 thick, ΔP=15 torr

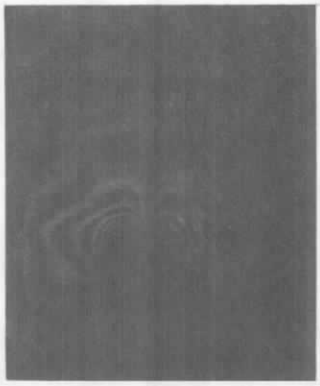

b. 1 inch separation, 2 ply specimen, 0.32" thick, ΔP=15 torr

Figure 6. The Effect of Specimen Thickness on Holographic Interferograms of Rubber/ Cord Specimens

of the specimen could not be detected. Cords which were broken after curing by means of a plunger could be detected in some cases. Breaking cords with this technique also has a tendancy to stretch and distort the specimens. Figure 7 shows an interferogram of one of these specimens. It would be difficult to predict that the fringe signature was that of a broken cord if the history of the sample were not known.

Figure 8 shows an interferogram of a specimen with a ply overlapped. The overlap is located in the center of the specimen and runs vertically from the bottom edge to the top edge. The fringe pattern seems to indicate an anomaly in the area of the overlap. This type of defect seems to manifest itself as an irregularity in the gross fringe pattern rather than a localized, high fringe density pattern which is indicitive of void and separations.

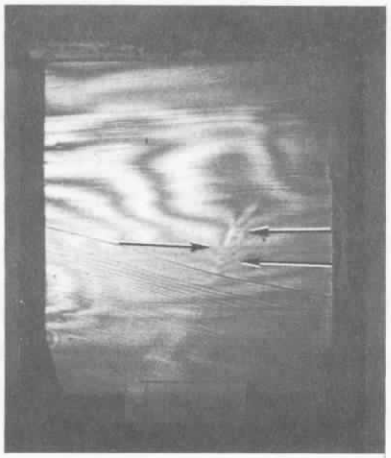

Figure 7. Holographic Interferogram of a Rubber/Cord Specimen with a Broken Cord

Figure 8. Holographic Interferogram of a Rubber/Cord Specimen with a Ply Overlap

2.3 CONCLUSIONS

Real-time holographic interferometric inspection of the rubber/cord control specimens provided the laboratory with valuable data and experience that was used as a baseline to advance to the succeeding phases of the program. The real-time technique allows the tester to view the dynamic effects continuously. As the straining vacuum pressure is applied, fringes generated by creeping rubber can be easily distinguished from those generated by surface displacement due to subsurface defects. The density of the fringe pattern generated by surface displacement caused by subsurface defects is directly related to the differential straining pressure. The greater the differential, the greater the fringe density. Separations and voids are usually identified by a localized fringe pattern. Excessive rubber and ply overlaps are usually identified by an irregular gross fringe pattern of rather low density.

The time dependence of creeping rubber is significant. If the creep rate is high, the fringe signature of an anomaly will not manifest itself and therefore remain undetectable. For specimens that were examined, it was found that a relaxation

time of 20 to 30 minutes was sufficient to allow the creep rate to diminish to the point that it no longer interfered with defect detection. The relaxation time required before pneumatic tires can be inspected will depend on the number of plies and tire size.

The optimum differential straining pressure required to expose most defects in the rubber/cord specimens varied from 15 to 40 torr. This variance depended on the types of defect and specimen composition and thickness. The optimum straining pressure required for automobile tire inspection can only be determined experimentally. The results from the rubber/cord specimens indicated that a 16 ply aircraft tire is certainly going to require a greater differential straining pressure than a 2 ply automobile tire.

3.0 DOUBLE EXPOSURE HOLOGRAPHIC STUDY OF TIRES PROGRAMMED WITH BUILT-IN DEFECTS

3.1 PROCEDURES

Special arrangements were made with major tire manufacturers to purchase 196 glass belted tires containing prescribed defects. The defects included separations in tread and sidewalls, weak bond sections surrounding a separation, permeable inner liners, broken cords, excessive ply overlap and deliberate out-of-roundness. The separations in most cases were created by using dabs of butyl-rubber cement. Cords were ruptured with a plunger after the tires were completely fabricated. Fifty-two of these tires have been holographically inspected and analyzed thus far.

In this phase of the program, the holographic inspection was performed using a GCO Model PT-12 Holographic Tire Analyzer. A description of this instrument and the procedures used are detailed in Appendix C. The tire analyzer was slightly modified by the addition of an etalon external to the laser cavity and by the elimination of some optical components. The addition of the etalon forces the laser to operate in a single mode. This increases the coherence length of the laser output and therefore eliminates optical components normally required to improve coherence properties of multimoded laser radiation. The elimination of these unnecessary components simplifies the optical alignment problems.

The GCO PT-12 constructs holographic interferograms of the inner surface of pneumatic tires by means of the double-exposure technique. The external straining force between exposures is applied by means of a differential vacuum pressure. This instrument generates a holographic interferogram of each quadrant of the tire and operates completely automatically throughout the entire inspection cycle. An auxiliary, laser illuminated, reconstruction setup is used to read and interpret the holograms. A tire defect map is made from the holographic information.

3.2 RESULTS

A summary of results is shown in Table 1. Typical holographic interferograms with characteristic signatures showing a tire with no defects and those with various types of defects are shown in Figures 9 through 21. Separations were detected readily. At the time of the writing of this report, failure analysis had not yet been completed on these tires. The failure to find all separations which the manufacturer was to have built into the tires does not necessarily indicate that any were missed. Under certain circumstances, even butyl rubber patches will not assure non-adhesion during curing. Other anomalies as out-of-roundness, and overlap of body ply were detected 50% of the time. Weak bond areas, ruptured cords and permeable inner liners could not be detected.

TABLE 1 SUMMARY OF DOUBLE EXPOSURE HOLOGRAPHIC STUDY

Group 1A

Number of Tires: 6

Type of Defect: Each tire had three separations of 1/2", 1" and 2" in diameter between the tread and top belt.

Results: All programmed separations were located and a good approximation of the separation size could be given. (Figure 10)

Group 1B

Number of Tires: 7

Type of Defect: Each tire had 3 separations of 1/2", 1" and 2" in diameter between the plies and the belt.

Results: All programmed separations were located and a good approximation of the separation size could be given. (Figure 11)

Group 2A

Number of Tires: 4

Type of Defect: Each tire had 3 separations of 1/2", 1" and 2" in diameter in the white sidewall area.

Results: 11 of the 12 programmed separations were located and the approximate size could be determined. (Figure 12)

TABLE 1 (Continued)

Group 2B

Number of Tires: 4

Type of Defect: Each tire had 3 separations of 1/2", 1" and 2" in diameter in the black sidewall area.

Results: 5 of the 10 programmed separations were detected and the approximate size could be determined. (Figure 13)

Group 3A

Number of Tires: 4

Type of Defect: 1" separation in the center of the tread area and a 1" separation in the white sidewall area. Separation were surrounded by a 12" weak-bond area.

Results: 6 of 8 programmed separations were located. The weak-bond area appeared to have no identifying signature. (Figure 14)

Group 3B

Number of Tires: 4

Type of Defect: 1" separation in the center of the tread area and 1" separation in the black sidewall area. Separations were surrounded by a 12" weak-bond area.

Results: 6 of the 8 programmed separations were detected. The weak-bond area appeared to have no identifying signature. (Figure 15)

Group 4

Number of Tires: 4

Type of Defect: Out-of-roundness from excessive rubber in the tread and shoulder area.

Results: This type of defect was detected in 2 of the 4 tires examined. (Figure 16)

TABLE 1 (Continued)

Group 5

Number of Tires: 5
Type of Defect: An overlap of 2" in the second body ply extending from bead to bead. (Figure 17)
Results: 2 of the 4 defective areas were located.

Group 6

Number of Tires: 4
Type of Defect: Second body ply was folded back on itself for 1" extending from bead to bead.
Results: 2 of 5 of these defects were located. (Figure 18)

Group 7A

Number of Tires: 4
Type of Defect: Ruptured cords in the center of the tread area.
Results: Careful inspection gave no indication of defects in the tread area. (Figure 19)

Group 7B

Number of Tires: 3
Type of Defect: Ruptured cords in the shoulder on the blackwall side.
Results: Careful inspection gave no indication of defects in the sidewall area. (Figure 20)

Group 8

Number of Tires: 3
Type of Defect: Permeable tubeless inner liner.
Results: No detectable defects in this area. (Figure 21)

3.3 CONCLUSIONS

From the data obtained, it appears that the technique of double-exposure holography in conjunction with a differential vacuum straining pressure is an excellent means for locating separations in pneumatic tires. Separations in the tread area could be detected in every case provided that the holograms were of average quality. Detecting separations in the sidewall area, especially in the wings of each quadrant, is slightly more difficult and requires good quality holograms for positive location. In the tread area, the observer is viewing the tire approximately normal to the inner surface of the tread area, whereas the sidewall region is viewed at a rather acute angle to the sidewall surface making fringe signatures of anomalies difficult to detect.

Tires which were out-of-round due to excessive rubber did manifest a detectable signature in some cases.

Cord ruptures and defective tubeless inner liners appear to have no identifiable fringe signature and are undetectable to holographic techniques (Figures 9 thru 21 are contained on the following pages; each figure page contains a detailed description of the photo above it.)

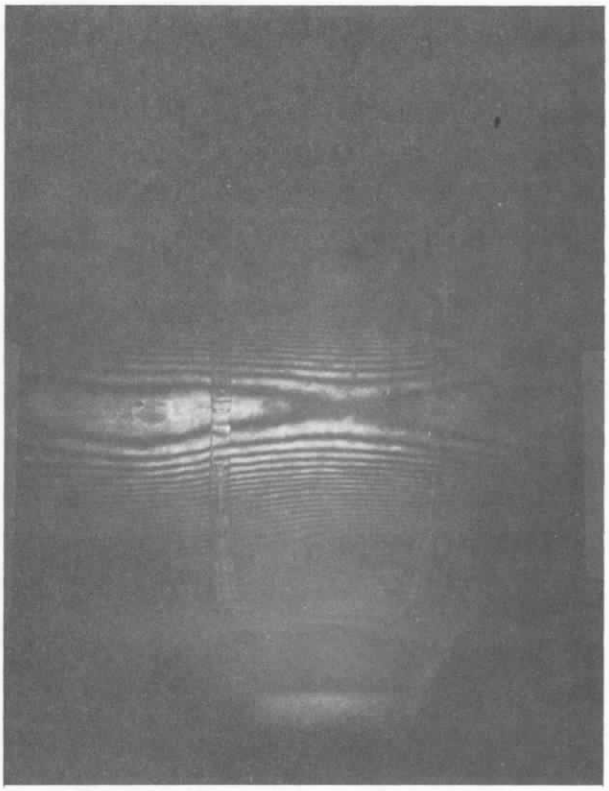

Figure 9. Holographic Interferogram of Tire with No Defects

Notes on figure:

The gross fringe pattern shown in the interferogram is typical of a tire with no defects. These fringes are the results of a uniform displacement of the inner surface of the tire about its entire circumference. The displacement is due to the application of the differential straining pressure to the air that is trapped within the fibers of the carcass cords. Notice that these fringes run in a circumferential direction and have no abrupt variations in the pattern which would usually be indication of an anomaly. Also in the hologram are the plastic marker bands which are placed at 30° intervals about the inner circumference of the tire to mark off sections of each quadrant for inspection. The bands also have marks to indicate 30° intervals in the radial direction. Defect locations can be easily pinpointed with the use of these bands.

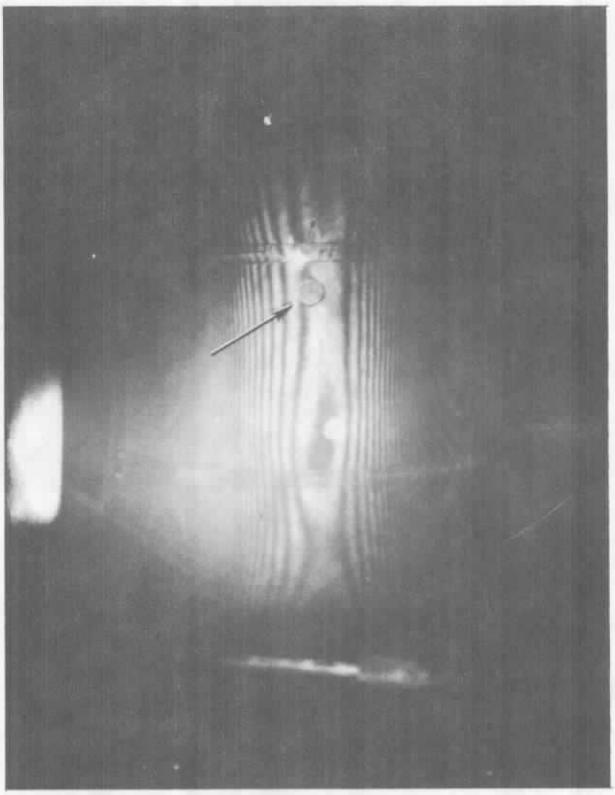

Figure 10. Holographic Interferogram of a Tire With a Separation Between the Tread and Top Belt.

Notes on figure:

The separation is indicated by the arrow. The fringe signature of the defect shows that the separation is circular in shape and approximately 1/2 inch in diameter. The low fringe density (7 fringes) can be an indication that the separation is not near the inner surface. This is true for this particular tire since the separation is between the belt and the tread.

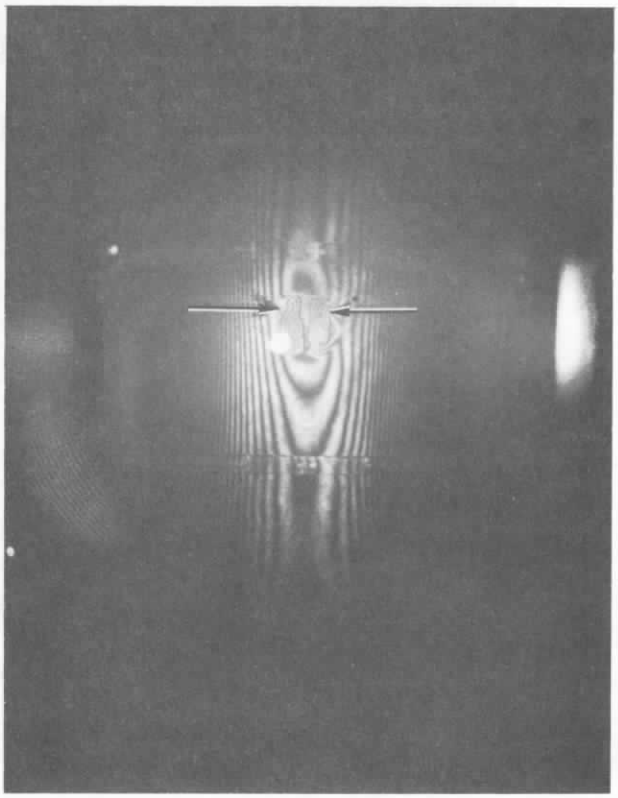

Figure 11. Holographic Interferogram of a Tire with a Separation Between the Plies and the Belt

Notes on figure:

This separation was programmed to be 2 inches in diameter. The interferogram shows that a narrow strip through the center of the separation bonded during the curing process resulting in two smaller adjacent separations as indicated by the arrow. The white spot in the photograph has no significance to the interferogram.

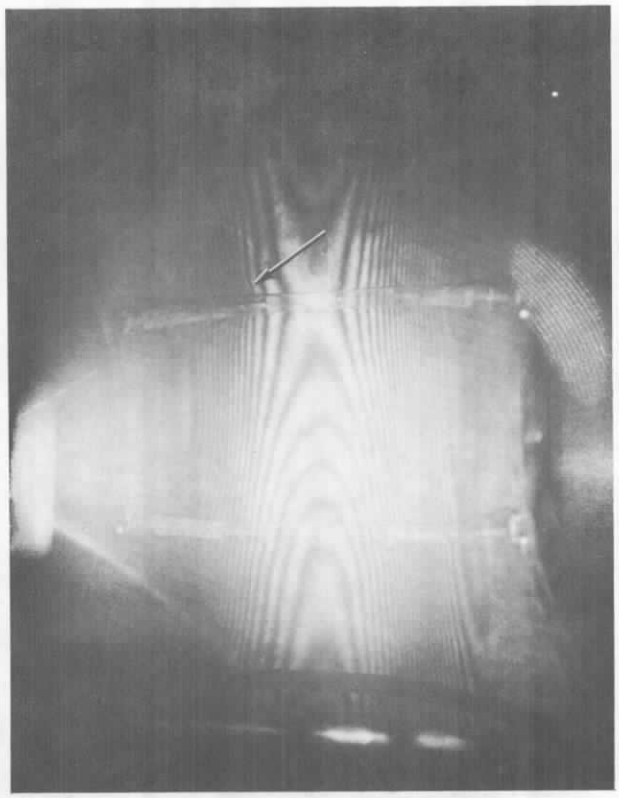

Figure 12. Holographic Interferogram of a Tire With a Separation in the White Sidewall Area

Notes on figure:

The separation location indicated by the arrow is slightly obscured by the plastic marker band. The fringe density is very high in the area of the defect and the individual fringes are not resolvable by eye in this photograph. The defect location is manifested by the termination of the gross fringe pattern in that area. The sidewall region of a tire is usually the most flexible part of the tire. Fringe signatures generated by separation located in the walls usually have a very high fringe density due to this flexibility.

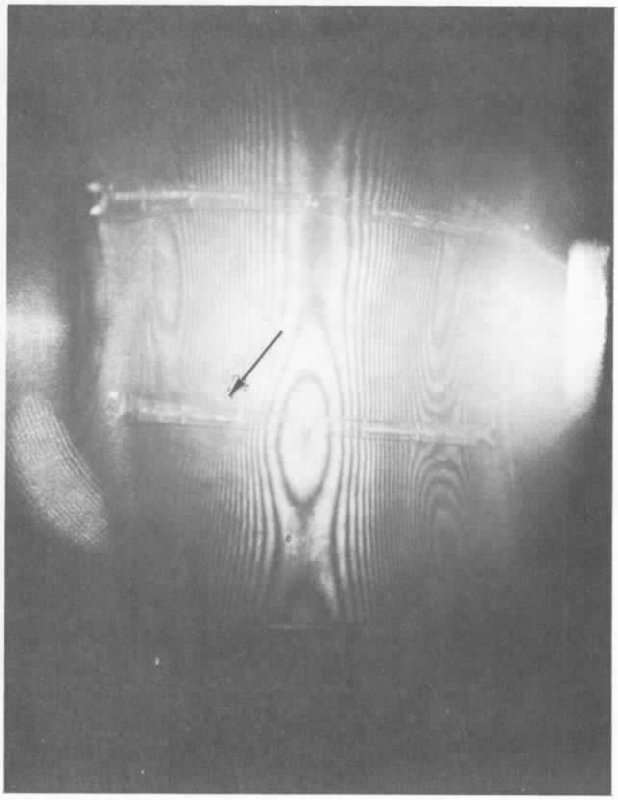

Figure 13. Holographic Interferogram of a Tire With a Separation in the Black Sidewall Area.

Notes on figure:

The separation location is indicated by an arrow and is partially obscured by the plastic marker band.

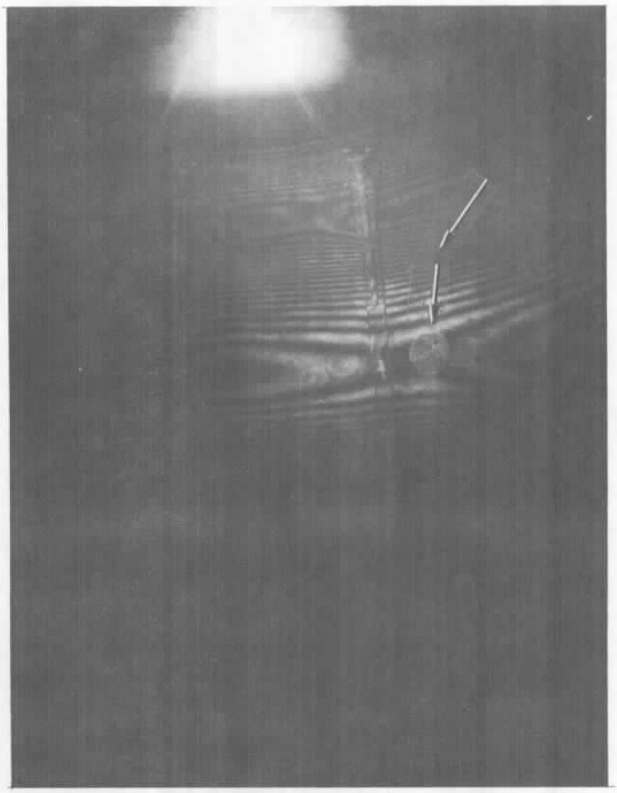

Figure 14. Holographic Interferogram of a Tire with a 1 Inch Separation in the Center of the Tread Area and a 1 Inch Separation in the White Sidewall Area

Notes on figure:

Arrows show the location of the separations. The interferogram does not appear to have any fringe signature which could be characteristic of a weak-bond. Tires of this type are intended to be wheel tested and periodically inspected between tests for possible propagation of the separations in the weak-bond area.

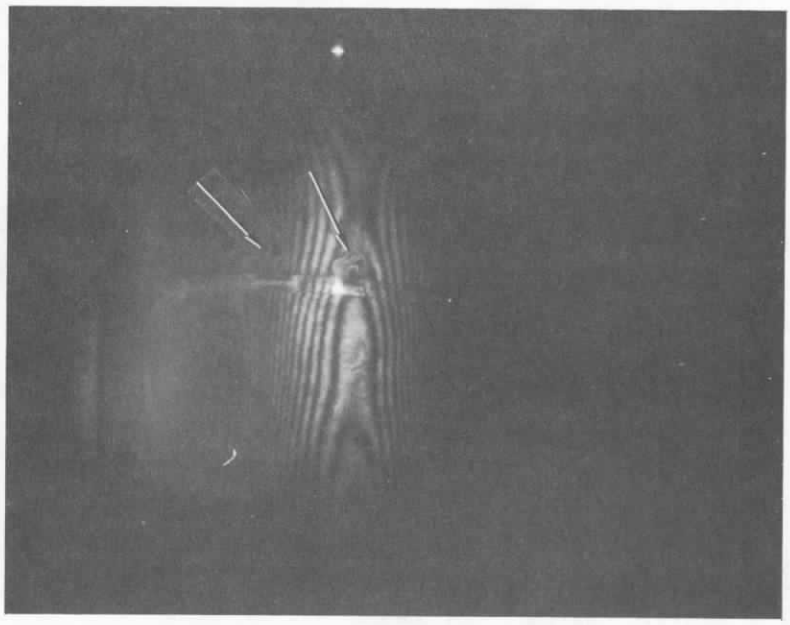

Figure 15. Holographic Interferogram of a Tire With a 1 Inch Separation in the Center of the Tread Area and a 1 Inch Separation in the Black Sidewall Area. Separations were Surrounded by a 12 Inch Weak-Bond Area

Notes on figure:

The arrows show locations of the separations. The weak-bond area was not identified.

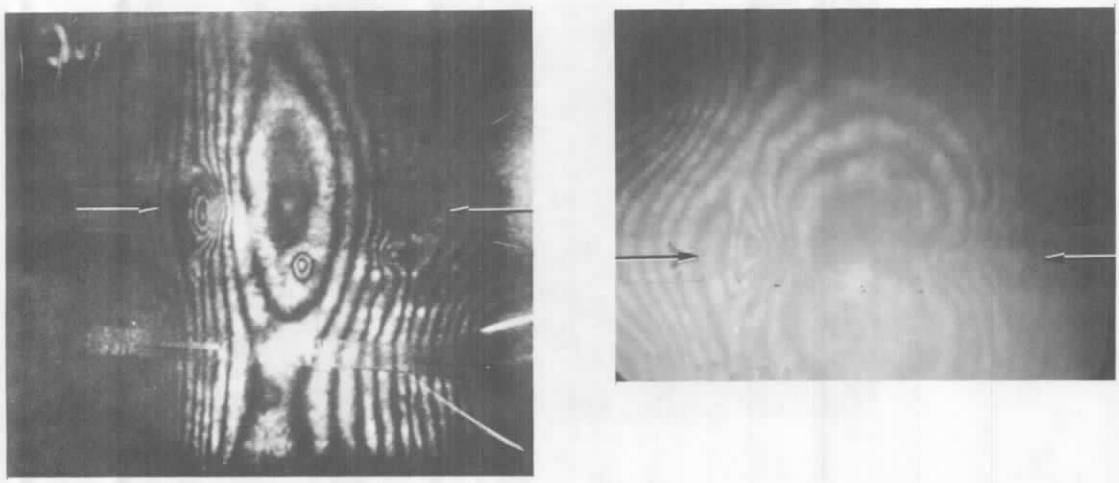

a b

Figure 16. Holographic Interferograms of 2 Tires Out-Of-Round From Excessive Rubber in the Tread and Shoulder Area

Notes on figure:

The distinct fringe pattern in Figure 16a shows air voids trapped in the area of the excessive rubber. Figure 16b shows a more subtle irregularity of the gross fringe pattern in the area of the excessive rubber containing no air voids.

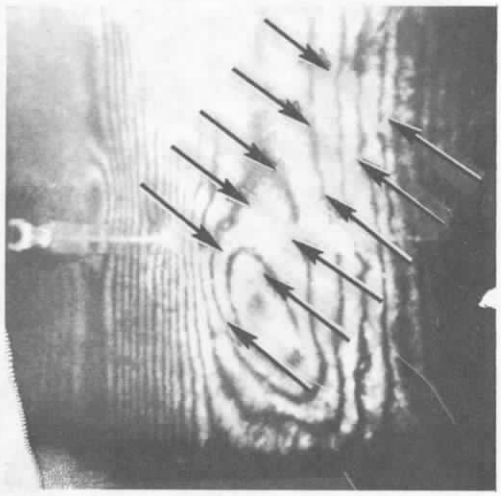

Figure 17. Holographic Interferogram of a Tire With an Overlap of 2 Inches in the Second Body Ply Extending from Bead to Bead

Notes on figure:

The arrows in the hologram show the area of the overlap. The fringe signature of this type ply overlap is characteristically an irregularity in the gross fringe pattern and runs across the tire at approximately 45°.

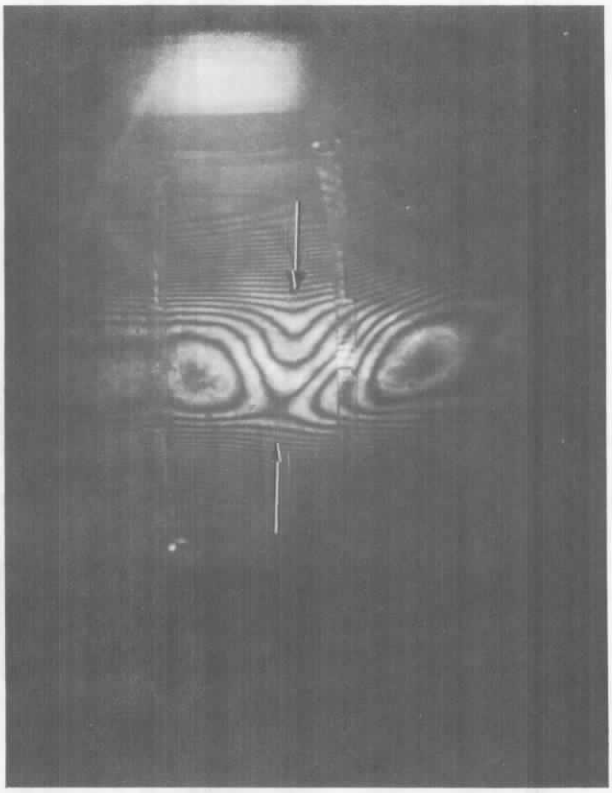

Figure 18. Holographic Interferogram of a Tire With Second Body Ply Folded Back on Itself for 1 Inch Extending from Bead to Bead

Notes on figure:

This type of defect can be identified by irregularities in gross fringe pattern.

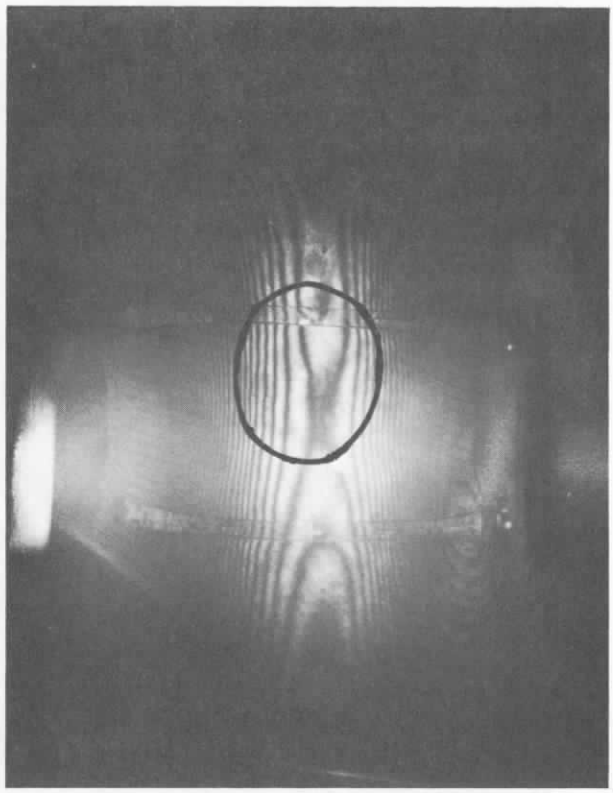

Figure 19. Holographic Interferogram of a Tire With Ruptured Cords in the Center of the Tread Area (No Defect Signature)

Notes on figure:

No unusual or irregular fringe patterns could be detected in the interferogram that might indicate an anomaly in the area. An X-ray picture of the area also failed to detect the broken cords. Location of the broken cords encircled.

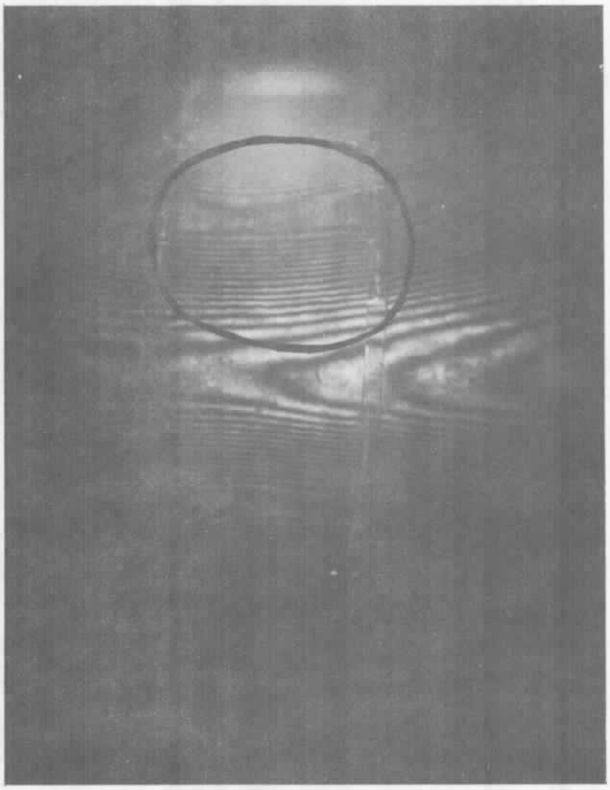

Figure 20. Holographic Interferogram of a Tire With Ruptured Cords in the Shoulder on the Black Sidewall (No Defect Signature)

Notes on figure:

The area in which the ruptured cord is located is circled in the hologram. No unusual or irregular fringe patterns could be detected in the interferogram that might indicate an anomaly in the area.

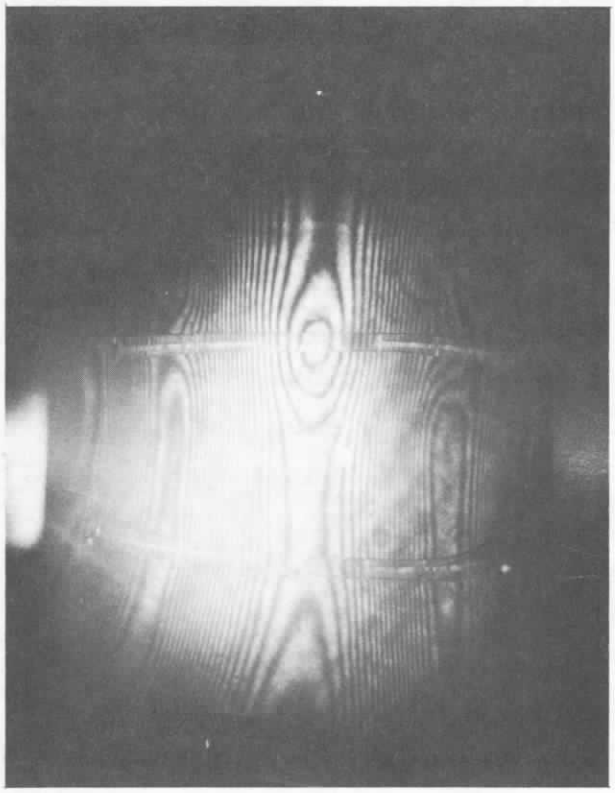

Figure 21. Holographic Interferogram of a Tire With a Permeable Tubeless Inner Liner (No Defect Signature)

Notes on figure:

This type of defect does not manifest a signature. Air cannot be trapped in the subsurface of the tire by this type of defect. For this reason, differential pressure straining techniques have no effect.

4.0 DOUBLE EXPOSURE HOLOGRAPHIC STUDY OF COMMERCIAL "OFF-THE-SHELF" TIRES

4.1 PROCEDURES

The fourth phase of the program is currently underway. Tires were purchased "off-the-shelf" on a random basis and examined holographically. The holographic findings were then compared with those findings made after each of the same tires were sliced and physically examined in minute detail.

Initially, this phase concentrated on locating separations with the intent that the experience gained and techniques developed and improved would be used later in the program to locate other types of defects which proved to be difficult to detect as shown in the third phase of the program. To date 112 new and retread tires have been examined holographically to detect separations. The results of this investigation are tabulated in this report. It is planned to expand these examinations to include detection of all types of defects in an additional 1000 tires, and these will be reported upon at a later date.

After purchase, all tires were first examined by the double-exposure holographic method using the GCO Model PT-12 Holographic Tire Analyzer. A description of this instrument and procedures used are detailed in Appendix C.

Upon completion of the holographic inspection and recording of the findings, the tires were tested dynamically under load for endurance or high speed in accordance with Motor Vehicle Safety Standard 109, New Pneumatic Tires, U.S. Department of Transportation Federal Highway Administration and National Highway Traffic Safety Administration. Upon completion of the dynamic tests, the tires were again examined holographically and results again re--corded.

The tires were then subjected to destructive analysis by sectioning. There were two major objectives to this analysis:

1. Using the reports of detected defects by the NDT procedures and their precise locations, the analysis attempted to find the cause of the NDT defect "signal".

2. To determine if the defect found during the first NDT inspection either propagates or relates to subsequent tire failure. Thus, the mode and mechanism of the failure or propagation was determined.

Each tire was carefully cut at the indicated defect position and also about an inch or more to each side, depending on the size of the defect. The rubber was peeled back from the cord and both examined under magnification for evidence of degradation by heat or abrasion. Since lack of adhesion between the cord and rubber is a major cause of defects, this aspect was given close attention.

A correlation was made between defects located holographically and those found by tire sectioning.

4.2 RESULTS

Holographic fringe signatures obtained on defective tires were typical of those obtained and described in Phase 3 of the program. Additional examples of fringe patternsn are included here. Figures 22 and 23 identify a ply separation. Figures 24 and 25 describe a tread separation. Figure 26 shows irregularities in the gross fringe patterns.

A total of 112 tires have completed the holographic inspection and failure analysis. The following results have been obtained thus far:

1. Number of tires in which both holographic and failure analysis found separations. - 91
2. Number of tires in which failure analysis found separations and holography did not. - 6
3. Number of tires in which holography indicated separations and failure analysis did not. - 15

At the beginning of the inspection program poor correlation between holographic detection of defects and failure analysis existed, but with experience and an improved marking system the correlation in detecting separations is currently running at

approximately 95%. Location of defects are now marked directly on the inner surface of the tires instead of using coordinates given by a defect map. Even with the improved marking system, separations of 1/4 inch diameter and smaller are sometimes difficult to find.

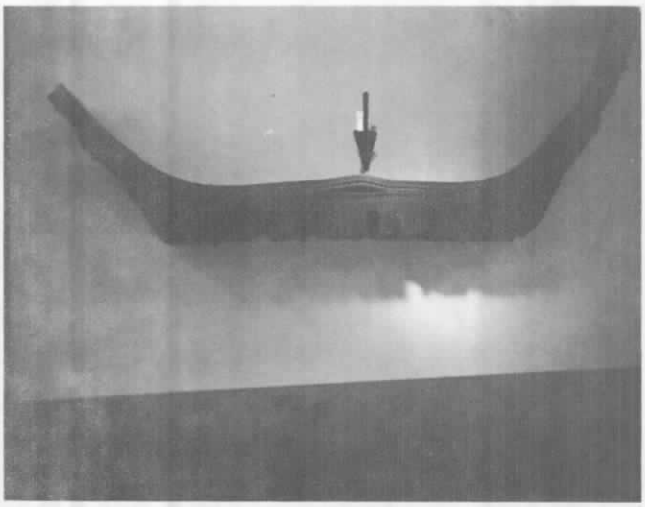

Figure 22. Section of a Tire (#ϕ1T6061) Carcass With a Ply Separation

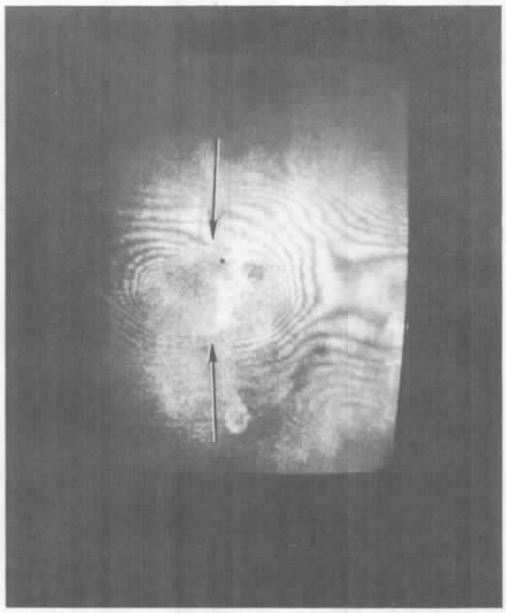

Figure 23. Holographic Interferogram of Tire (#ϕ1T6061)

Notes on figures:

Figure 22 is a photograph of a section of a tire which has a separation between the plies of the carcass. Figure 23 is an interferogram of that portion of the tire. The arrows show the location of the separation. Notice that the fringe density of this type of separation is very high. This is typical for separations between the inner plies which are near the inner exposed surface of the tire.

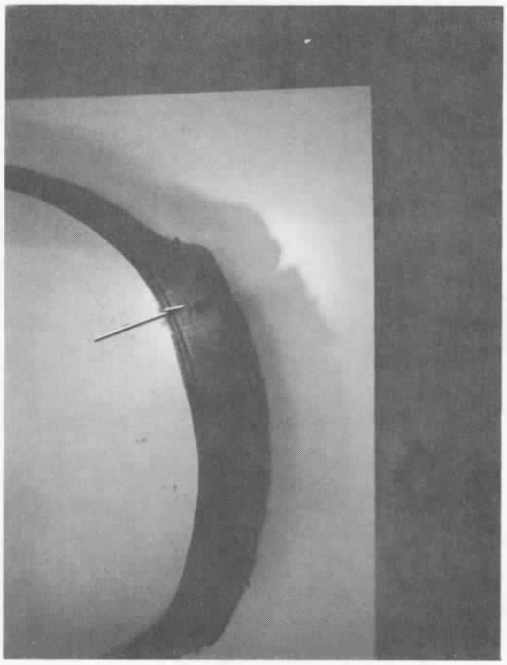

Figure 24. Section of a Tire (#ϕ1T6142) Carcass With a Tread Separation

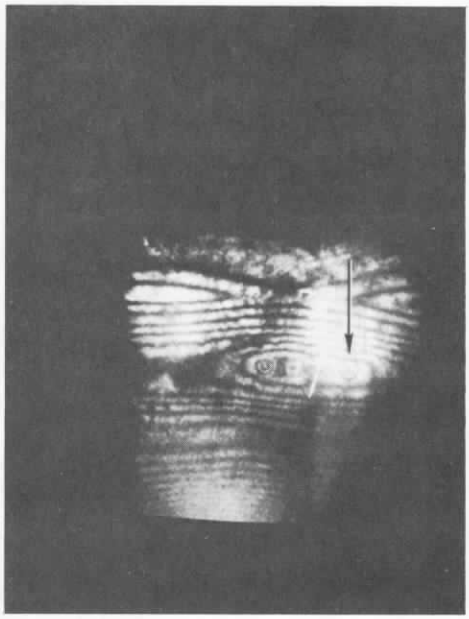

Figure 25. Holographic Interferogram of Tire (#ϕ1T6142)

Notes on figures:

Figure 24 shows a photograph of a section of a retreaded tire which has a separation at the junction of the new tread rubber and the old carcass rubber. This is a defect commonly found in failed retread tires. Figure 25 is an interferogram of that same portion of the tire. The arrow locates the position of the separation. Notice that the fringe signature of the separation contains only a few fringes. This is usually an indication that the separation is not near the surface exposed to holographic exposure.

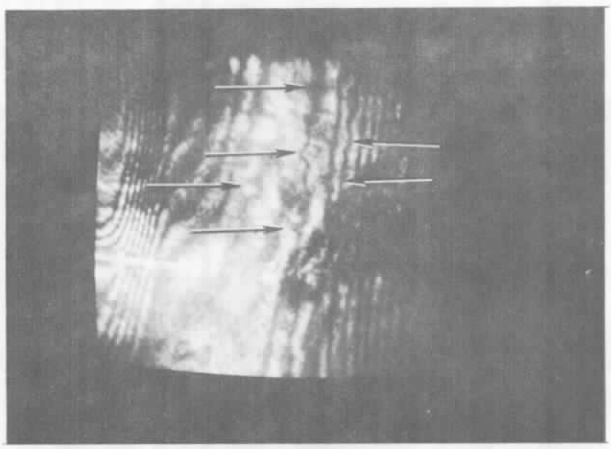

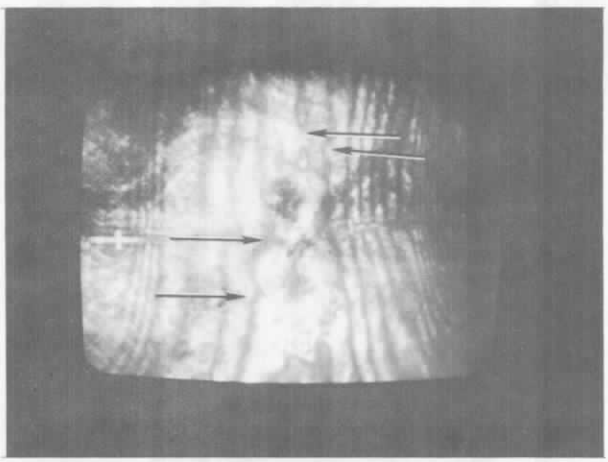

Figure 26. Irregularities in Gross Fringe Pattern

Notes on figure:

The interferograms in Figure 26 show irregularities in the gross fringe pattern. Tires exhibiting this type of signature have failed during wheel tests. Studies are currently underway to identify the anomaly.

4.3 CONCLUSIONS

As experience was gained in the program, separation locations predicted from the holographic inspection of tires correlated very well with the separations found from tire sectioning by the Failure Analysis Laboratory.

Holographic inspection identified hidden defects in some tires which had passed the MVSS 109 compliance test. Failure Analysis also uncovered these same defects and reclassified the tires as "failed".

Location of defects other than separations requires improvements in instrumentation and techniques which are currently being pursued by the NDT Laboratory at the Center. It is planned to continue the program with the examination of many more tires. Results of this effort will be published at a later date.

5.0 DISCUSSION

A thorough study of the state of the art established the course and objectives of this holographic tire inspection work. With that as a baseline, the experience gained in the study, and the data obtained and its correlation with identified defects, we are reasonably assured that holographic inspection is a good method for nondestructively detecting separations in pneumatic tires.

The holographic inspection method, with some additional refinements in equipment and technique, also appears to offer a good approach to detecting other types of defects such as weak-bonds, ply overlaps, ruptured cords and out-of-roundness. Additional work is being pursued at this laboratory to improve holographic inspection technqiues using essentially the same equipment with minor modifications so that these "other types" of defects can be located and identified with greater assurance than established thus far in this study. Additional tires will be examined and reported on at a later date to verify the application to these other type of defects.

The GCO PT-12 holographic inspection system which was used extensively in this study will be used in the next phase of the program as a basis for improvement of techniques by the modification of the existing instrument.

The GCO PT-12 uses the vacuum differential straining technique which appears to be the superior straining technique and is the key factor to successful assurance in locating and identifying defects in tires by holography.

As for time required to make a holographic inspection, the GCO tire analyzer is capable of inspecting a tire in approximately 2-1/2 minutes. This does not include preparing the tire for examination or hologram processing and analysis. One operator inspects about 20 tires per day. A three or four man operation can increase the inspection rate to 100 to 150 tires per day. This rate is generally adequate for laboratory or factory prototype inspection but certainly not for production line outputs.

State of the art laser technology along with modern holographic techniques could certainly improve the inspection rate of existing holographic tire inspection systems. A rate of one tire inspected every 30 seconds does not seem unreasonble. Replacing the commonly used cw laser with a pulsed ruby laser would solve many of the problems. Ruby laser systems are now available with coherence properties and repetition rates required for a high rate holographic inspection. Very little tire preparation would be required. A double-exposure hologram, generated by a double-pulsed ruby system (a few seconds between pulses) would contain very few creep fringes even though the tire was not allowed to relax. Environmental vibration and disturbances are no longer a problem so that the time allowed for vibrational damping in existing cw laser system is eliminated.

The feasibility of holographically inspecting mounted tires has been studied by various laboratories. The holographic techniques required for recording inspection interferograms of external surfaces of tires are available. The major problem with inspecting mounted tires is deciding which straining technique to use. Vacuum straining techniques have proved to be an excellent means for loading tires between exposure, but the vacuum method cannot be used on inflated tires. Straining by mechanical vibrations or inflation pressure changes appear to be the most logical techniques that can be applied. A great deal of data is available that was generated by using these techniques in conjunction with holographing the external surface of tires. These data show that only major defects are detectable. If the minor defects that are not detectable do not lead to tire failure, then this technique would be adequate. Unfortunately, this correlation has not yet been made. Analysis and correlation of data being complied here at TSC should answer some of these questions.

Almost all the holographic interferograms generated in non destructive testing are recorded on photographic emulsion. Some recent work has been done using a video camera and video storage devices. This system stores the holographic information in a video storage device and then can be viewed at any time on a cath-

ode-ray tube. Interferograms generated in the preliminary investigations were not of good quality but the system does show a great deal of promise and flexibility.

Regardless of the recording technique, hologram reading and analysis in the past has been done visually by an operator. Apparently very little has been done in the field of pattern recognition for the reading and analyzing of interferograms. One technique that has been used with some success is the hologram correlation technique. In this method, the hologram acts as an information filter. The amount of light the hologram transmits is a direct measure of the amount of interference generated by the hologram. This technique has been used with some success in studying plain and uncomplicated objects, but does not appear to be sophisticated enough to detect defect fringe patterns in very complicated interferograms that are generated by pneumatic tires. If completely automatic holographic inspection systems are to be realized, then this is certainly an area where much work needs to be done.

6.0 RECOMMENDATIONS

The holographic inspection of commercial pneumatic tires currently underway is intended to assess the economic and reliability of tire defect detection using holographic methods. The result indicate that the method is reliable for experiment. Based upon these results it is recommended that work be performed in the following areas:

a. Improve the accuracy of detecting separations, and improve the productivity of existing equipment through minor modifications of equipment and advanced techniques.

b. Improve holographic recording techniques and hologram analysis so that defects other than separations can be reliably detected.

c. Determine the degree of correlation between tire failure and anomalies detected holographically.

APPENDIX A

REVIEW OF BASIC OPTICAL HOLOGRAPHY AND HOLOGRAPHIC INTERFEROMETRY

HOLOGRAPHY

Figure A-1 (a) is a basic holographic setup used for generating holograms. In this setup, a laser output beam is split into two beams, the reference beam and the object beam. The reference beam illuminates the photographic plate and the object beam illuminates the object being holographed. Light scattered from the object forms a wave front characteristic of the object's surface and form and interacts with the reference beam at the photographic plate and generates the hologram. The hologram can be reconstruted and viewed using only the reference beam and the original geometry of the construction setup (see Figure A-1b). The construc-

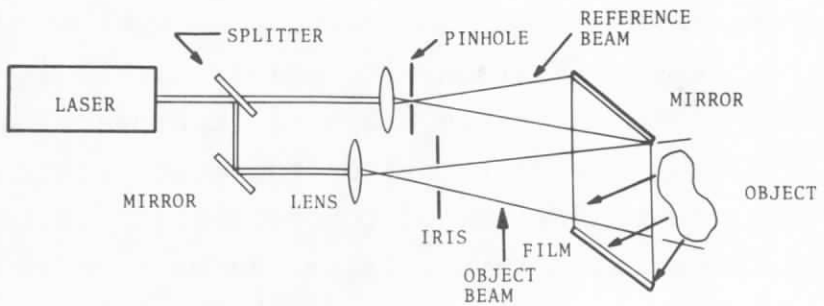

(a) HOLOGRAPHIC RECORDING

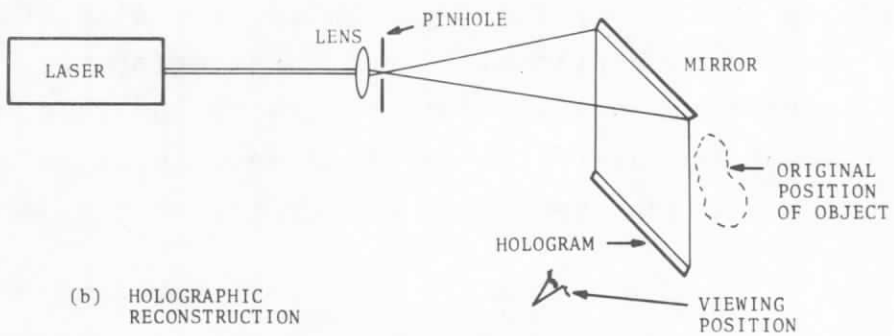

(b) HOLOGRAPHIC RECONSTRUCTION

Figure A-1. Typical Holographic Set-Ups

tion system must have good mechanical and thermal stability. The wavelength of the light source used for generating the hologram should be the same as that used for reconstruction so as to maintain the original size of the object and to minimize aberations and distortions.

A hologram can be considered a recording of a system of interference fringes which is a representation of the interference of two wave fronts. When the hologram is properly illuminated, the wavefront is reconstructed and the original scene can be viewed exactly as it existed. Both the recording and the reconstruction of the hologram require a coherent light source. The property of coherence can be described as a phase property of the light beam. This coherence property can be divided into two parts, temporal coherence and spatial coherence. Temporal coherence is the time relationship within the beam. Consider the light beam as being generated by hundreds of individual oscillators and that all the generators are in phase. The individual beams would then be in phase with each other and the total beam output would have good temporal coherence. A light beam with good spatial coherence must have the property that any two points within the illuminated field can be made to interfere. Spatial coherence is a prerequisite for uniform fringe formation and good fringe contrast.

The requirements for a good coherent light source can be met with a laser, especially if the laser can be made to operate in a single mode (TEM_{oo}). This greatly enhances the point to point reconstruction within a hologram.

HOLOGRAPHIC INTERFEROMETRY

A new type of interferometry has been developed using the properties of the wavefront generated from a reconstructed hologram. In the conventional Michelson interferometer, a monochromatic light beam is split into two parts and then beat back together so as to interfere, creating an interference fringe pattern. Any disturbance within either arm of the interferometer

produces a shift in the interference fringe pattern. The disadvantages of this interferometric technique is that the object under investigation must be transparent or highly reflective and optically flat.

In holographic interferometry, wavefronts from two holograms on the same plate or from a hologram and the illuminated holographed object are superimposed, thus generating an image of the object. If the object has been distorted or displaced after the first hologram exposure has been taken, interference fringes are generated in the area of the distortion in the reconstructed image. The number of interference fringes is a direct measure of the topographical changes of the object. If no changes take place, no fringes are generated and only the holographic image is present. With this technique, very complex objects can be examined regardless of their surface reflectivity or shape.

REAL-TIME HOLOGRAPHIC INTERFEROMETRY

In real-time holographic interferometry, a single exposure hologram is made in its static position. The photographic plate is then either developed and replaced to its exact original position or developed in place. The interference between the wavefront from the holographic reconstructed image and the wavefront from the laser illuminated object is then observed. Any variation made on the surface of the object can be viewed in real-time. A permanent record can be made with a conventional camera.

DOUBLE EXPOSURE HOLOGRAPHIC INTERFEROMETRY

A double-exposure hologram is constructed by taking two holographic exposures on the same photographic plate held in a static position. The object under investigation is stressed or strained between exposures. Any variations on the surface of the object will appear as interference fringes in the reconstructed image. This technique produces a permanent record of the topography of the object and can be viewed or photographed with a conventional camera when illuminated with visible laser radiation.

APPENDIX B

REAL-TIME HOLOGRAPHIC INTERFEROMETRIC APPARATUS AND PROCEDURES TO INSPECT CONTROLLED SPECIMENS

This appendix describes the instrumentation and procedures used for the real-time studies of rubber/cord control specimens. Figure B-1 is a schematic of the holographic system.

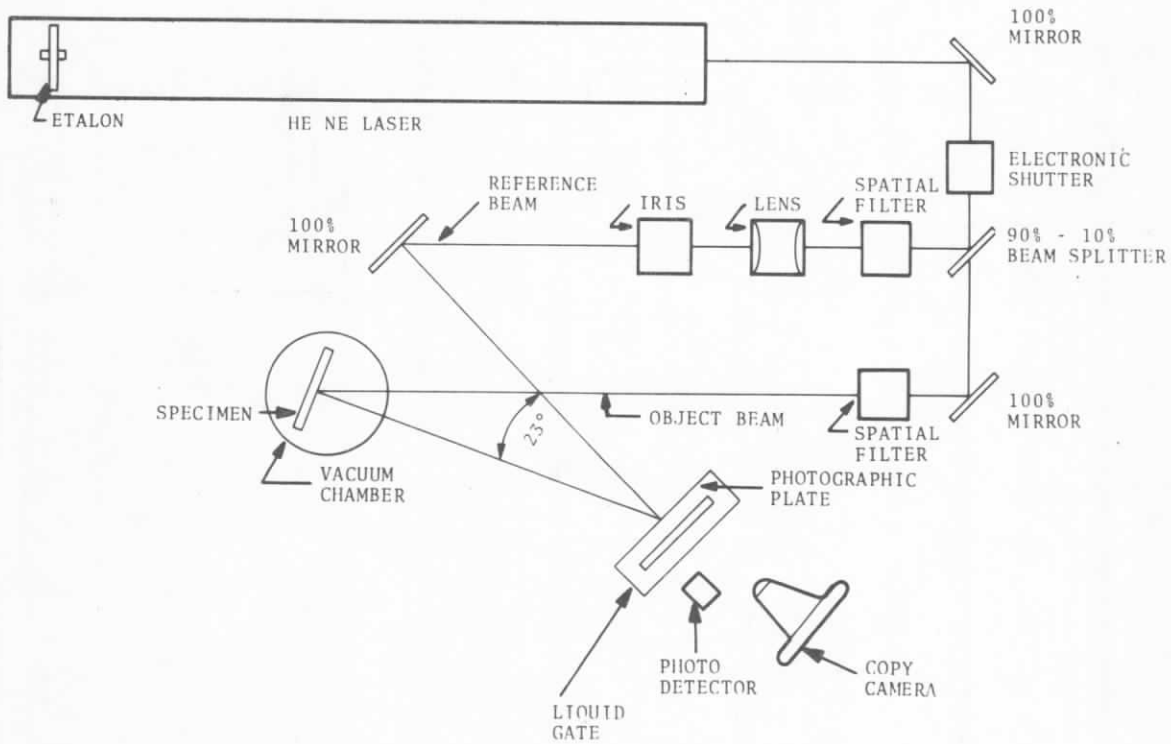

Figure B-1. Real-Time Holographic Interferometer Schematic

Figure B-2 is a block diagram of the setup and shows the manufacturer and model number of each component. Figure B-3 shows the laboratory equipment in place.

The light sources used is a Spectra Physics Model 125 Helium Neon Laser. This laser contains an intercavity etalon which forces the laser to operate in a single mode (TEM_{oo}). The laser output is about 50 milliwatts at 6328 Å. The output beam passes

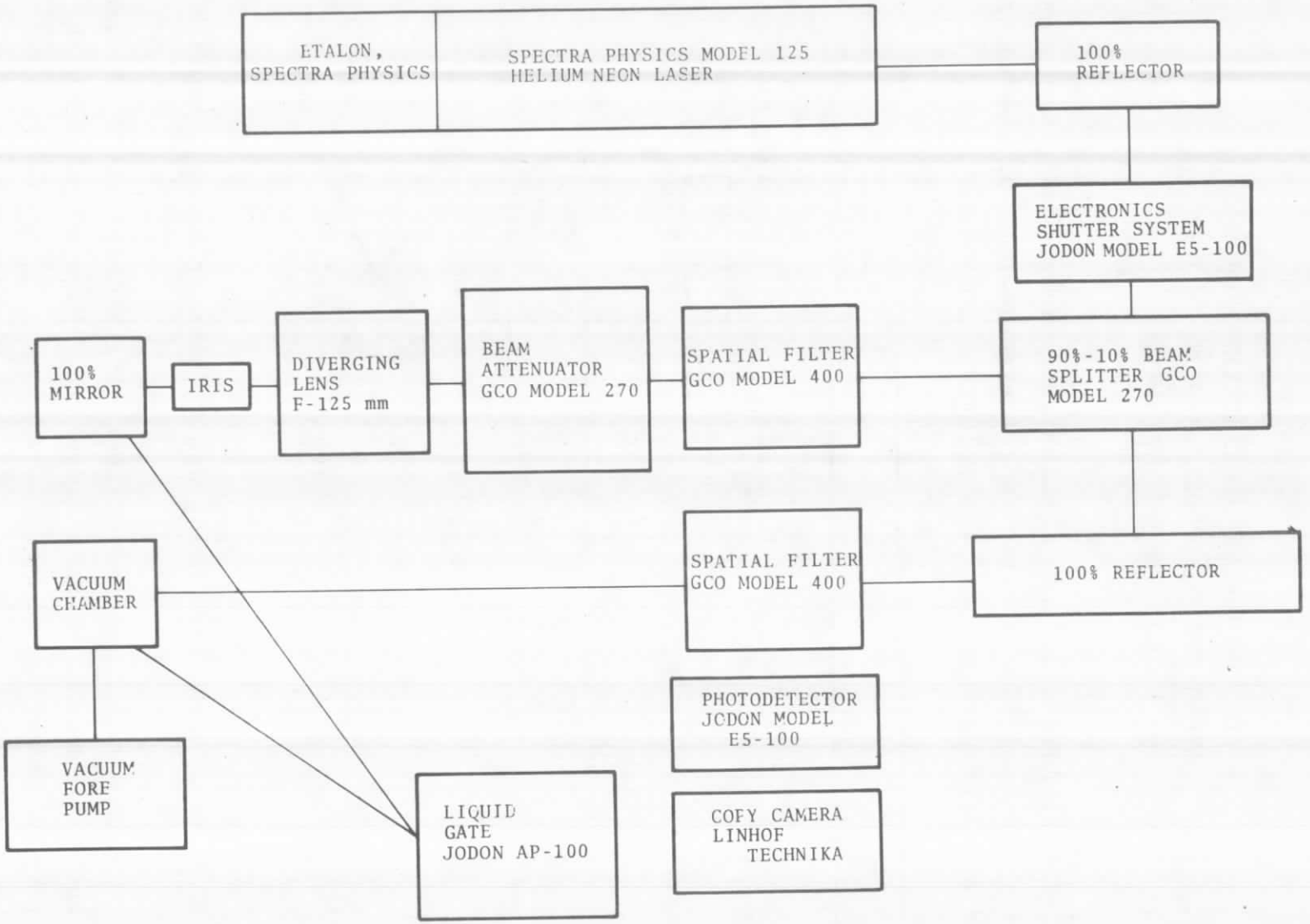

Figure B-2. Block Diagram of the Real-Time Holographic Interferometric Set-Up

through an electronic shutter operated by an automatic electronic system so that the photographic plates receive the proper exposure. A photodetector is placed in front of the photographic plate and sees the same radiation which is incident on the plate. The photodetector monitors the radiation so that the exact exposure (ergs/$_{cm}$2) can be assured.

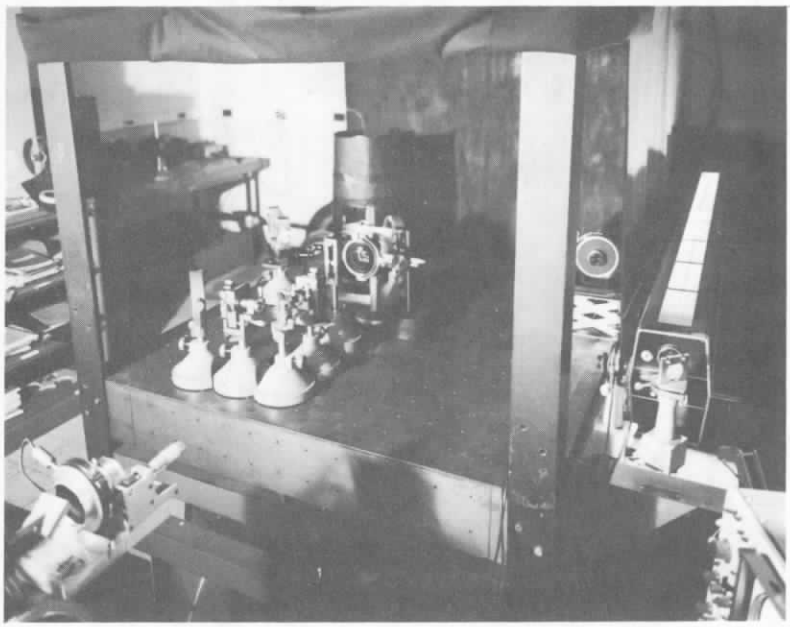

Figure B-3. Laboratory Real-Time Holographic Set-Up

Other minor optical components in the system are lenses, reflectors and spatial filters. The 100% reflectors are used to direct the beam through the various components of the system. A 10% reflecting and 90% transmitting beam splitter is used to split the main beam into the reference and object beams. The ratio of the reference beam to the object beam at the photographic plate is about 5 to 1. The beam attenuator in the reference beam is used to control this ratio. The spatial filters improve the

quality of the beam, and modes which are detrimental to good hologram generation are filtered out of the system. A diverging lens is used in the system to expand the reference beam so that the entire photographic plate is illuminated.

In the real-time study of the rubber/cord specimens, the straining force used was a partial vacuum. The specimens were placed in a vacuum chamber (Figure B-4) and an exposure made at

Figure B-4. Vacuum Chamber and Specimen Holder

atmospheric pressure. The plate was processed in place producing a hologram of the specimen. A partial vacuum was then applied to the specimen. If the specimen contained a subsurface separation, the adjacent surfaces were displaced slightly or bulged out due to the pressure differential between the trapped air in the separation and the partial vacuum inside the vacuum chamber. A displacement of the surface can be detected viewing the object through the hologram. The object must be illuminated by the object beam and

the reference beam must illuminate the hologram. The hologram acts as an interference filter and fringes are generated if any surface displacement has taken place.

Figure B-5a is an interferogram of a specimen which has no defects. Only a gross fringe pattern is present. Figure B-5b is an interferogram of a specimen with a one inch separation in the center. The concentric fringe pattern indicates the location and size of the separation. Dynamic changes can be viewed as the straining pressure is varied. Photographs of the interference pattern can be taken with a conventional camera if a permanent record is desired.

As mentioned above, the exposed photographic plates are processed in place. Any displacement of the plate after exposure will result in unwanted interference fringes in the reconstructed image. A displacement of 1/2 wavelength produces one fringe.

Another photographic plate processing technique involves the removal of the exposed plate, processing it and replacing it at its original position to within one wavelength. This can be a very difficult operation.

In the "processing in place" technique, the photographic plate is held securely in position by a liquid gate (photographic plate holder). The liquid gate serves two purposes, (1) to hold the plate and (2) to form a liquid tight enclosure about the plate so that the plate can be photographically processed without having its original position disturbed. Figure B-6 shows the liquid gate and the electronic control console. The liquid gate is displayed with the top open and the photographic plate protruding about 1/2". When in operation, the photographic plate is pushed down into the gate (cell) and the lid is secured forming a water tight cell. The cell has windows on both sides and is connected to the control unit through two hoses. For holographic recording, a photographic plate is placed inside the cell and the lid is secured. The cell is filled with water and the plate is allowed to soak for several minutes to allow a good optical match between the plate and the windows. The plate is then exposed. It is now ready to be processed and the automatic processor is put into

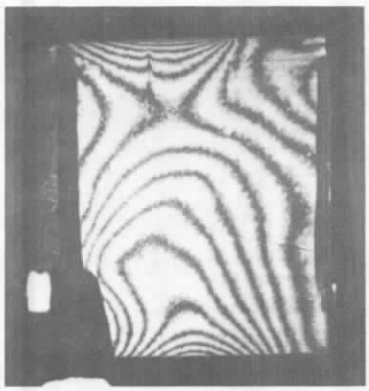

(a) Rubber/Cord Specimen with No Defects

(b) Rubber/Cord Specimen with a 1 Inch Separation

Figure B-5. Holograms of Rubber/Cord Specimens

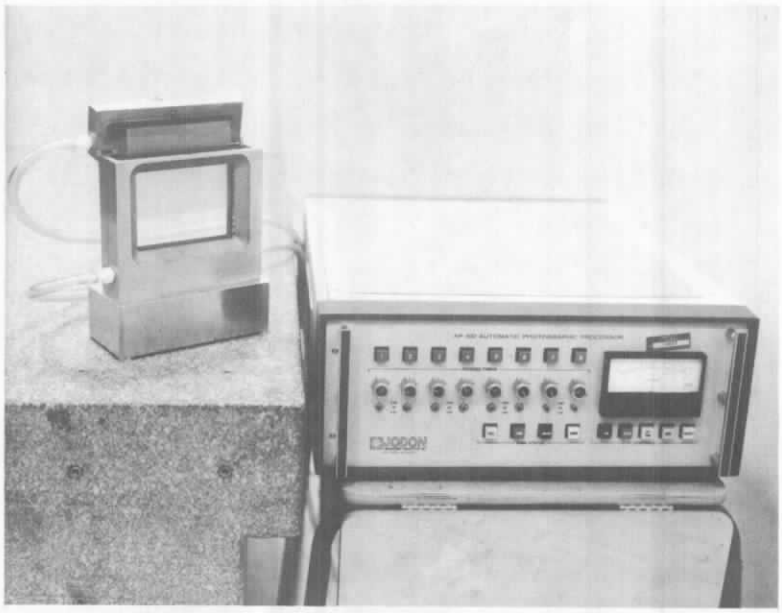

Figure B-6. Automatic Film Processor and Liquid Gate

operation. The developing solution, stop bath and fixer solution are fed into the cell in the proper sequence. Once the developing cycle has been completed, the plate is flushed several times with clean water. The cell is then filled with water. The hologram is now ready to act as the interference element for the interferometric viewing of the specimen.

APPENDIX C

DOUBLE-EXPOSURE HOLOGRAPHIC APPARATUS AND PROCEDURES USED TO INSPECT TIRES

The GCO Model PT-12 Holographic Tire Analyzer was used to inspect the series of tires with programmed defects and in the inspection of a group of tires which were purchased "off the shelf" in the open market.

Figure C-1 is a photograph of the tire analyzer. The instrument produces double-exposure holographic interferograms in conjunction with the vacuum differential straining technique. The tire analyzer holographs the inner surface of the tires and can be operated in a completely automatic mode. The basic principle of the technique is that two exposures are made of each quadrant of a tire, one exposure at atmospheric pressure and one exposure in a partial vacuum. If a separation exists in the quadrant, the air trapped in the separation will force the adjacent surfaces to bulge out. In the reconstructed image of this hologram, fringes are generated in the area of the separation. The fringes are caused by an interference between the two holograms generated from each exposure on the same photographic film.

Figure C-2 is a simplified schematic of the optical system used in the tire analyzer. The holographic light source is a Spectra Physics Model 125 Helium Neon Laser which has an output of about 50 milliwatts when operating in a single mode (TEM_{oo}). The etalon used in the system was not furnished with the tire analyzer and is a modification made at the TSC Tire Testing Laboratory. Without the etalon in the system, the laser has a multimoded output and in general has poor coherence properties. The optical shutter located adjacent to the laser is electronically controlled by a photodiode in the film plane and assures the proper exposures. Reflectors direct the laser beam from the laser through a window in the dome flange into the vacuum chamber. Here the beam is split into the reference and object beams. Lenses are used to expand the beams so as to illuminate the inner surface of

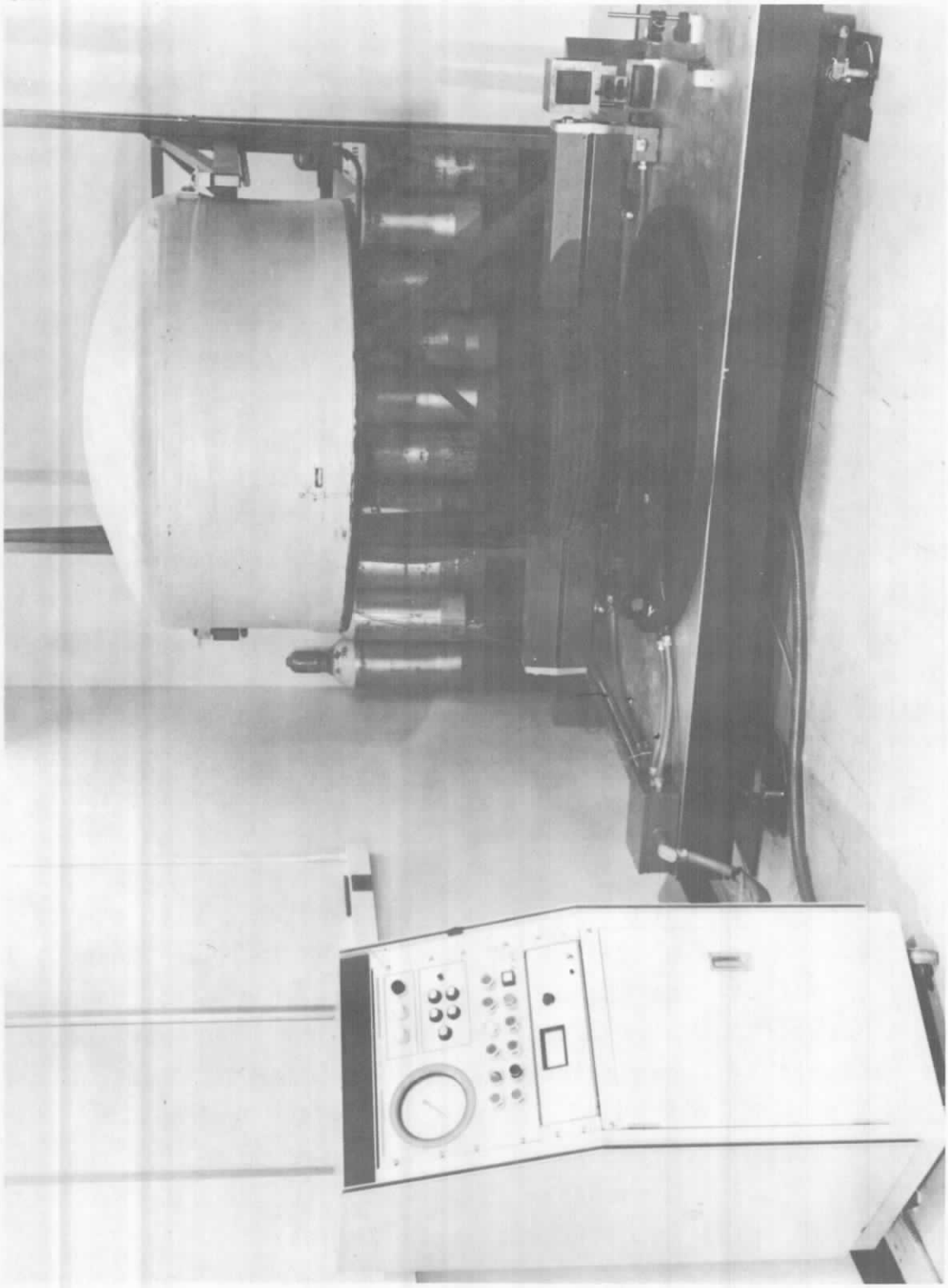

Figure C-1. GCO PT-12 Holographic Tire Analyzer

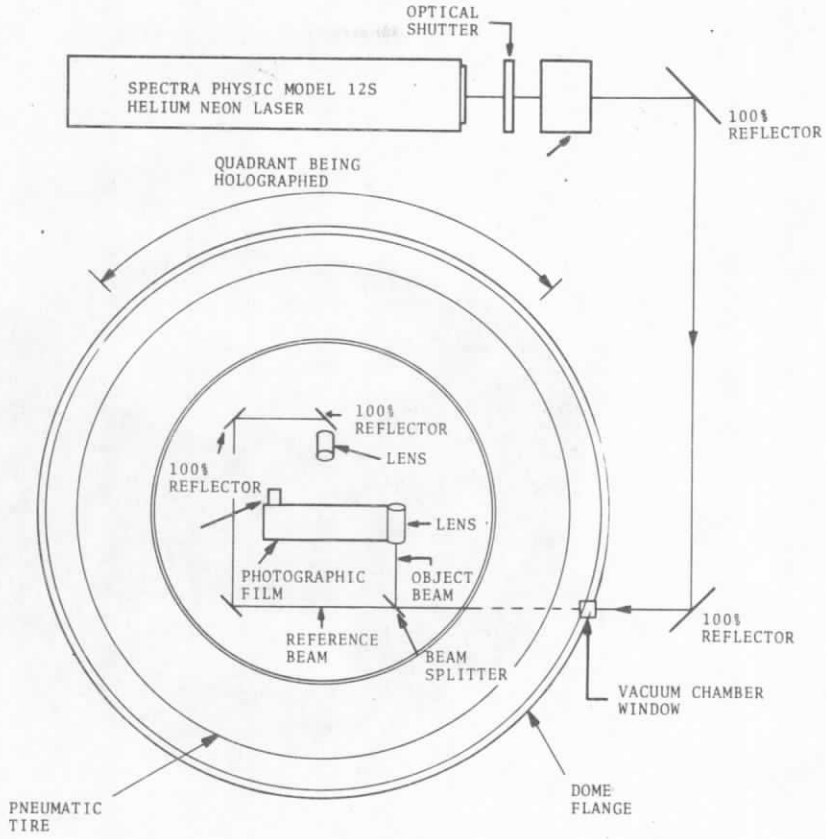

Figure C-2 Shematic of Optical System of GCO Holographic Tire Analyzer

the tire and the photographic film. This system uses 70mm film (10E75) as the recording medium. The film is handled and controlled automatically by a film cassette which holds enough film to inspect about 15 tires.

Tires are prepared for inspection by first inserting four tire spreaders (see Figure C-3) across the tire beads at 90° intervals around the tire. The spreaders force the beads apart and make the inner tire surface more accessable for holographic inspection. A light coat of white talc powder is sprinkled on the inner surface to make it more reflective thereby reducing exposure times and improving hologram quality. Tires are allowed to relax in the spread position for at least 20 minutes before they are loaded into the tire analyzer. This relaxation allows the creeping of the rubber to subside. The tire is placed on a rotating table and sidearms are pressed against the tread of the tire so as to secure the tire and minimize vibrations (see Figure C-4). The

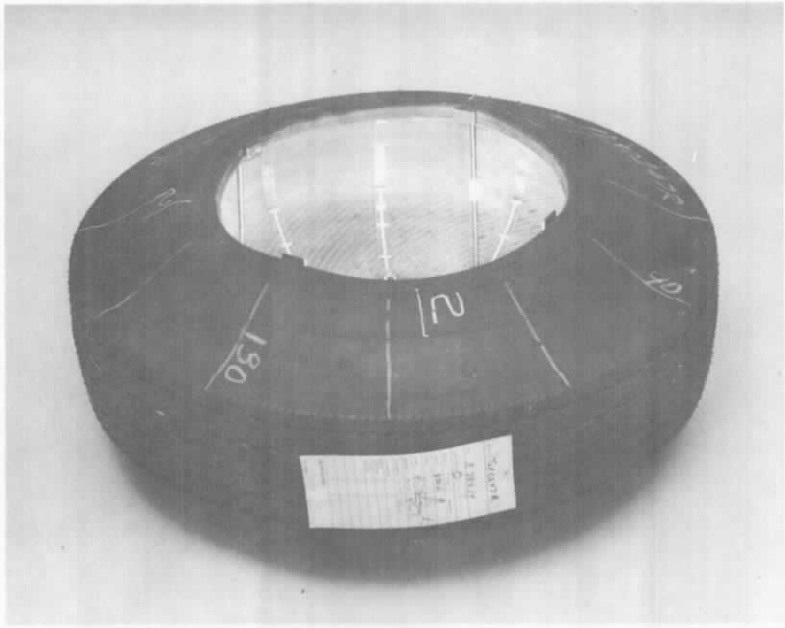

Figure C-3. Tire Prepared for Holographic Inspection

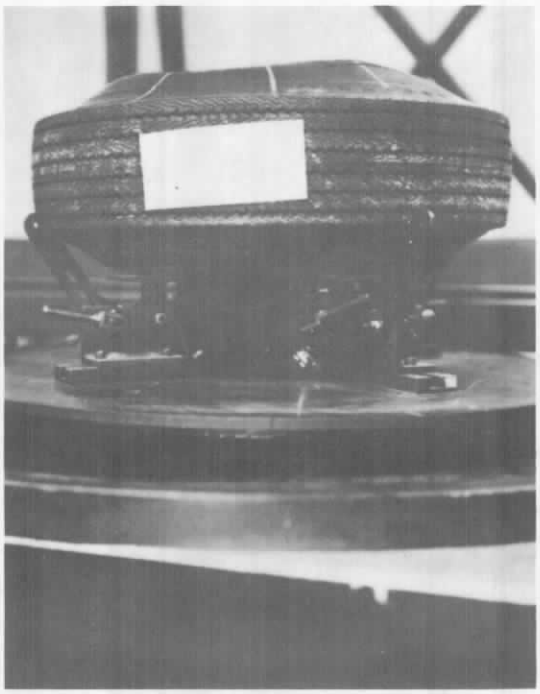

Figure C-4. Turn Table and Sidearm Mounts

tire analyzer is supported by pneumatic supports and is fairly isolated from any environmental disturbances. Once the tire is securely in place, the automatic inspection cycle is started. The cycle begins with the lowering of the dome to form an sealed chamber. The dome rests on a flange and forms a vacuum tight seal. The film is advanced and one exposure is taken at atmospheric pressure. A partial vacuum is pulled on the chamber and a second exposure is made of the same quadrant of the tire. The film is then advanced and the tire is rotated 90° so that the next quadrant is in position to be holographed. This procedure is repeated until the four quadrants have been inspected. The cycle is then terminated with the lifting of the dome. Several seconds elapse between each function to allow vibrations to dampen. The inspection for one tire requires approximately 2-1/2 minutes.

The photographic film is processed using standard developing chemicals with no special care necessary. Holograms are reconstructed and analyzed using an auxiliary reconstruction setup, (Figure C-5), which uses a Spectra Physics Model 124 Helium Neon

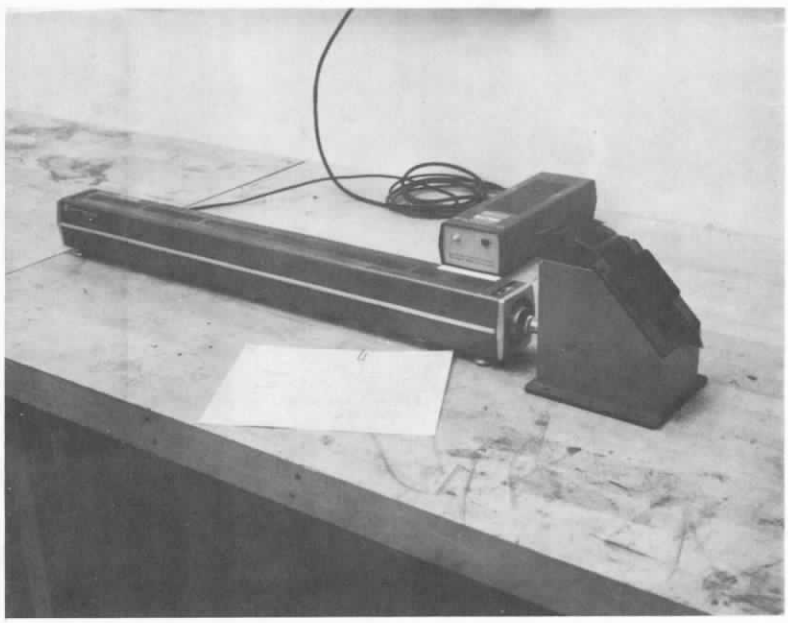

Figure C-5. GCO Holographic Reconstruction Setup

Laser as the light source. The optical magnification and geometry is the same as that used by the GCO Tire Analyzer. This is necessary so that original sizes are maintained and aberrations minimized. Holograms are read by an operator and defects maps of the tire inner surface are constructed.

Figures C-6, C-7, and C-8 are typical interferograms generated by the tire analyzer.

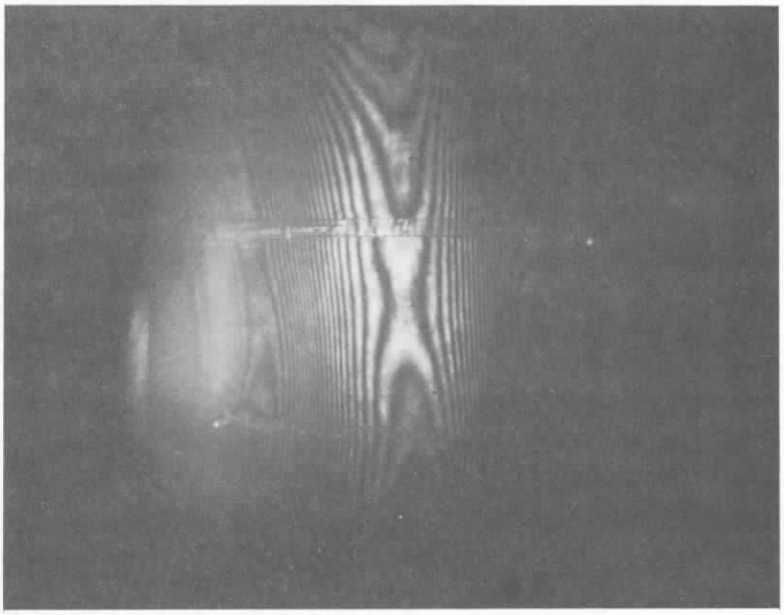

Figure C-6. Holographic Interferogram of a Tire with No Defects

Notes on Figure:

This is an interferogram of tire with no defects. Only a gross fringe pattern is visible which is the result of a uniform displacement of the inner surface of the tire about the entire circumference. The displacement is caused by the application of the differential straining pressure to the air that is trapped within the fibers of the carcass cords. Notice that these fringes run in a circumferential direction and have no abrupt variations in pattern. Also in the hologram are the plastic marker bands which are placed at 30° intervals about the inner circumference of the tire to mark off sections of each quadrant for inspection. The bands also have marks to indicate 30° intervals in the radial direction. Defect locations can be easily pinpointed with the use of these bands.

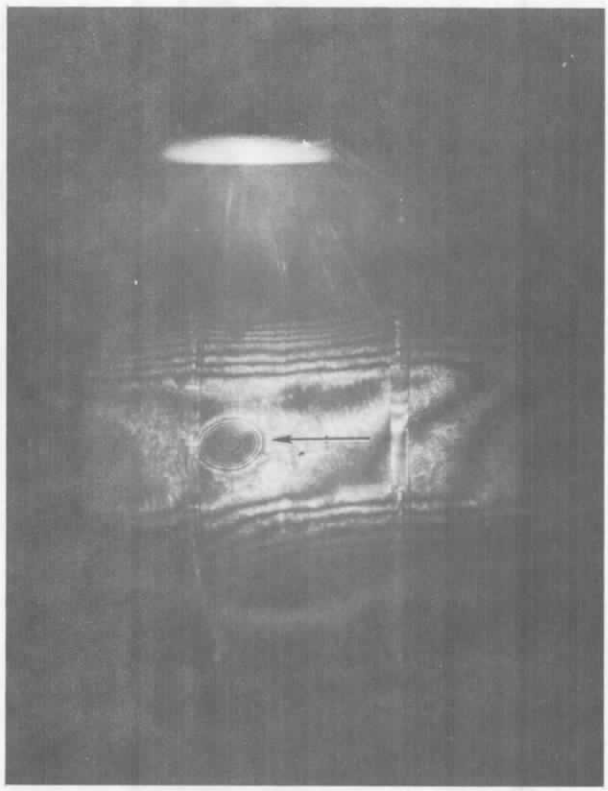

Figure C-7. Holographic Interferogram of a Tire with a Separation Between the Tread and Top Belt

Notes on figures:

The separation is indicated by the arrow. The fringe signature shows the separation to be circular in shape and approximately 1 inch in diameter. The low fringe density (6 fringes) can be an indication that the separation is not near the inner surface. This is true for this particular tire since the separation is between the belt and the tread.

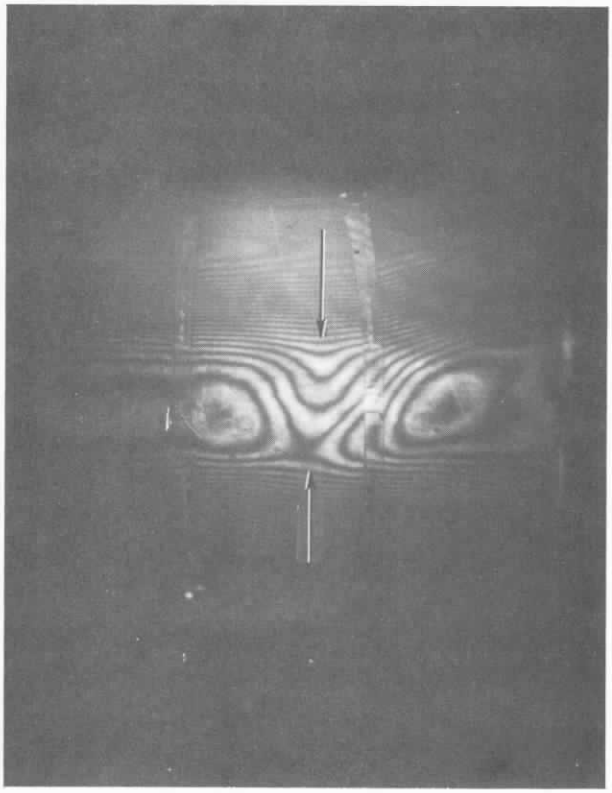

Figure C-8. Holographic Interferogram of a Tire with a Ply Overlap

Notes on figures:

This interferogram shows a fringe signature of a ply overlap, the arrow indicating the area of the defect. This type of defect can be identified by an irregular gross fringe pattern.

APPENDIX D

GLOSSARY AND SYMBOLS

Aberrations - Phase errors on a light wave which forms the image of a point

Beam Splitter - An optical element which reflects one portion of incident light and transmits the remainder

Coherence Length - A measure of the temporal coherence of a light source (in essence, the maximum difference in optical path at which time invariant interference can occur)

Exposure - The amount of light energy per unit of the area which strikes a photographic film

Laser - Acronym for "light amplification by stimulated emission of radiation," a source of highly coherent, monochromatic light

Mode - A radiation filled pattern which is independent of time (a laser which oscillates in a single transverse mode emits spatially coherent radiation)

Object Beam - The light which is scattered or transmitted by the object to the hologram

Phase - A property of a sinusoidal oscillation which describes the portion of a cycle completed at any given instant

Reference Beam - Light which is added to the object beam to form a hologram

Spatial Coherence - A measure of the degree of phase correlation at two different points illuminated by the same light source, primarily determined by the width of the light source

Spatial Filter	- Selective extraction of information which is encoded by spatial modulation of a light wave
Temporal Coherence	- A measure of the degree of phase correlation with time between two fixed points along a given ray direction
TEM_{oo}	- The lowest order single transverse mode that has a gaussian distribution of intensity across the aperture.
cw	- Continuous wave

78178